DETECTION OF FECAL CONTAMINATION IN APPLE CALYX BY MULTISPECTRAL LASER-INDUCED FLUORESCENCE

A. M. Lefcourt, M. S. Kim, Y. R. Chen

ABSTRACT. *Feces is a suspected source of contamination of apples by disease-causing organisms such as* E. coli *O157:H7. Laser-induced fluorescence imaging was used to detect applications of 20 μL of 1:20 or 1:200 dilutions of dairy cow feces to the calyx of Red Delicious apples. Detection of the 1:20 dilution was 100% even after washing the apples. Detection of the 1:200 dilution was more difficult, and no sign of contamination was seen for 25% of the apples, presumably because the petals on the calyx screened the small contamination sites. For the other 75% of the 1:200 treated apples with visual signs of contamination, about 75% of the contamination sites could be detected before washing and 58% after washing. These findings suggest that the calyx, with its petal structure, will hinder detection of very low levels of fecal contamination on apples, but that moderate levels of contamination equivalent to about 150 ng of dry matter can easily be detected.*

Keywords. *Apples, Food safety, Imaging, Measurement techniques.*

Bacterial pathogens introduced into the food chain can cause disease and are thus an important human health issue (Armstrong et al., 1996; Buchanan and Doyle, 1997; Brackett, 1999; Mead et al., 1999). The presence of hemolytic *E. coli* bacteria, and particularly the O157:H7 strain, in unpasteurized apple juice has been linked to a number of cases of serious illness, including death (Steele et al., 1982; Besser et al., 1993; CDC, 1996, 1997; Cody et al., 1999). Feces from animals, and in particular from cattle and deer, are thought to be the primary vector for bacterial contamination of fruit juices (Lang et al., 1999; Riordan et al., 2001; Uljas and Ingham, 2000), and the federal government has issued a directive in an attempt to reduce fecal contamination of juices (FDA, 2001).

In response to this federal directive, the USDA Instrumentation and Sensing Laboratory at Beltsville, Maryland, instituted a program to develop rapid, noninvasive methods to detect fecal contamination of apples. In prior studies, we demonstrated that the fluorescence response of feces to UV excitation is a very sensitive marker for the detection of fecal contamination of apple surfaces (Kim et al., 2002b), that use of a pulse laser for excitation allows detection under ambient lighting conditions (Kim et al., 2003b), and that approximately 15 ng of diluted feces applied to the cheek sides of Red Delicious apples could be detected using laser-induced fluorescence imaging techniques (Lefcourt et al., 2003, 2005). The calyx is the most heterogeneous area of apples in terms of physical structure and coloration, e.g., the petals of the sepal can obscure or hide potential contamination sites. This study examined the ability and sensitivity of a multispectral laser-induced fluorescence imaging system to detect diluted feces applied to the apple calyx.

Article was submitted for review in December 2002; approved for publication by the Information & Electrical Technologies Division of ASAE in July 2005.

Company and product names are used for clarity and do not imply any endorsement by the USDA to the exclusion of other comparable products.

The authors are **Alan M. Lefcourt, ASAE Member Engineer,** Research Biomedical Engineer, **Moon S. Kim,** Research Physicist, and **Yud-Ren Chen, ASAE Member Engineer,** Research Agricultural Engineer, Henry A. Wallace Beltsville Agricultural Research Center, USDA-ARS, Beltsville, Maryland. **Corresponding author:** A. M. Lefcourt, Henry A. Wallace Beltsville Agricultural Research Center, USDA-ARS, Bldg. 303 Powder Mill Rd., Beltsville, MD 20705; phone: 301-504-8450; fax: 301-504-9466; e-mail: alefcour@anri.barc.usda.gov.

MATERIALS AND METHODS

FECES

Fresh feces from individual cows were collected at the Beltsville Agricultural Research Center (BA) and at the University of Maryland (UM) Clarksville dairies. Feces were collected using 50 mL polypropylene vials and stored at 4˚C for up to 2 d prior to use. Feces were diluted 1:20 or 1:200 by weight using double-distilled water. In addition, samples of feces were dried to a constant weight at 65˚C to determine dry matter percentages, which were 15% for BA and 14% for UM feces.

APPLES

The Red Delicious apples were handpicked at the Rice Fruit Co. orchards (Gardners, Pa.) and were stored in a refrigerated storage room maintained at 3˚C. Intact, rot-free apples were selected randomly for treatment. Treatment was applied to 10 apples for each dilution and feces source. With two dilutions by two sources, a total of 40 apples was used in the study.

TREATMENTS

A single 20 μL drop of 1:20 or 1:200 diluted feces (equivalent to approximately 150 or 15 ng of dry matter, respectively) was applied to the calyx next to the sepal region. To allow for flow of particulates, about 4 mm was cut off the pipette tips. In most cases, the application spot was at least partially obscured by sepal petals. Measurements (see below) were made 1 d and 7 d after treatment. Between measurements, apples were stored in the apple refrigerator. After the 7 d measurements, the apples were tumble washed

and returned to the refrigerator. A third set of measurements was made 1 d after washing.

For tumble washing, random groups of 10 apples were placed in a rectangular bucket containing clean water at 10˚C. The apples were manually tumbled for 60 s prior to being moved to a second bucket kept under running water. The running water caused the apples to tumble naturally. Again after 60 s, the apples were removed, held for a moment to allow most of the water to drip off, and then placed on clean cardboard trays.

Imaging System and Acquisition

The multispectral, laser-induced fluorescence imaging system consisted of a pulse laser (frequency-tripled Nd:YAG emitting at 355 nm, 10 Hz, 125 mJ per pulse, Quanta Ray, Spectra-Physics, Mountain View, Cal.), a beam expander, an *f*1.4/35 mm Nikon lens, a common-aperture multispectral adapter (MSAI-04, Optical Insights, Tucson, Ariz.), and a fast-gated intensified camera (1280 × 1024, 12-bit, 20 ns minimum gate width, Dicam-Pro, Cooke Corp., Romulus, Mich.). The laser beam was expanded via a divergent lens (CVI, Albuquerque, N.M.) to illuminate a target area approximately 30 cm in diameter at a distance of 200 cm from the laser. The common-aperture multispectral adapter uses a series of prisms to convert a target area into four equal-sized images (640 × 512) and includes a four-filter holder where individual one-inch filters can be readily changed. Filter parameters used for this study were: 30 nm FWHM at 450 nm (blue band), 40 nm FWHM at 550 nm (green band), 22 nm FWHM at 678 nm (red band), and 10 nm FWHM at 730 nm (far-red band). See Kim et al. (2003b) for a more detailed description of the imaging system.

Images were taken of individual apples. After a few measurements were made, it appeared that the position of the apple affected the fluorescence response of apples treated with the 1:200 dilution of feces. Thus, for the measurements made 1d after treatment, a sequence of four images was taken for each apple with the apple rotated 90˚ perpendicular to the axis of the calyx between images. Markings were added to the apples to indicate the four positions so that the same positioning could be used on subsequent days. The position that yielded the greatest response on day 1 was the only position imaged on subsequent days. Reflectance images were also taken on day 1 for a single position using a diffuse white light source.

Image Processing

A computer program was written in Visual Basic (version 6, Microsoft, Redmond, Wash.) to convert the 1280 × 1024 images into four 640 × 480 individual band images. The individual images were geo-spatially registered so that images from the four bands could be directly overlaid or ratioed; where necessary, black columns or rows were added to the edges of images. A second program was written to allow visualization and analyses of individual band images as well as images constructed using ratios or linear combinations of band images. The general scheme for identifying contamination sites was to enhance images to emphasize a contamination site, use a binary threshold filter to isolate the attribute associated with the contamination site, and then overlay the detected area or areas onto the original image for visual conformation. If enabled, the number of discrete areas detected (based on a selected maximum distance between positive pixels in the binary image) and the number of positive pixels within each detection area were listed. Automated classification of a detection area as a contamination site was based on comparison of calculated centroids of positive pixels within the detection area with values in a look-up table. The look-up table was constructed manually by classifying centroids based on observations of overlaid detection areas. The detection process could be automated so that any number of tests, each using any permutation of image enhancements, could be applied to all apples and the results printed to a text file; images with detection information could also be printed. A third program was written to tabulate detected areas of individual images and to allow application of selected detection thresholds to differentiate contamination sites from non-specific responses based on the number of positive pixels within a detection area.

Detection Algorithms

After preliminary tests with a number of types of potential image enhancement techniques (e.g. non-linear scaling, and morphological and convolution filters), a generalized analysis sequence was selected for detailed testing (table 1). For each step in the analysis sequence, a specific enhancement (Weeks, 1996) was selected from a list of potential enhancements. Step 0 in the analysis sequence addressed the relative advantage of spatially binning images prior to analyses. Step 1 addressed effects of noise and effects of small, natural, variations in apple surfaces by use of an averaging filter. Step 2 addressed the question of the value of using gradient methods to detect contamination sites. Step 3 addressed potential problems resulting from differences in illumination intensity by scaling images based on histograms of image intensity. Linear correction factors were used to scale images to 8-bit images or, equivalently, to scale detection thresholds. The correction factors were based on two points in the cumulative histograms of individual image intensities. The lower point was not critical, as at least 20% of an image was black background. For individual images, the intensity level corresponding to the lower 5% histogram level was mapped to an intensity of 20. For the upper point, two different strategies were used; the upper point represented either the median intensity of an image or the near-maximal intensity of an image. For the median option, the level of intensity corresponding to the 50% histogram level was mapped to an intensity of 60. For the maximal intensity option, 99% was mapped to 200. For step 4, the gray-scale image was converted to a binary image using a manually selected image conversion threshold. Step 5 consisted of no filter, shrinking the binary image by negating any positive pixel with a non-positive 8-neighbor, or smoothing the image by negating any positive pixel where six or more 8-neighbors were non-positive. Subsequently, all positive pixels within a selected distance of each other in the binary image were classified as belonging to the same detection area. A detected area was categorized as a “contamination” site if the number of positive pixels within the area was greater than the detection threshold. The detection threshold could be set manually, or automatically to exclude all false negatives based on the largest number of positive pixels detected in a “false positive” detection area.

Table 1. Sequence of potential enhancements applied to images. One enhancement was selected for each step.

Sequence	Enhancements
Step 0:	A. No binning
	B. 2 × 2 spatial binning
Step 1:	A. No filter
	B. 3 × 3 averaging filter
	C. 5 × 5 averaging filter
	D. 5 × 5 Gaussian filter
Step 2:	A. No filter
	B. 3 × 3 Prewitt filter
	C. 5 × 5 Prewitt filter
	D. 5 × 5 Sobel filter
Step 3:	A. No scaling
	B. Linear scaling based on median image intensity
	C. Linear scaling based on maximal image intensity
Step 4:	A. Binary threshold filter
Step 5:	A. No filter
	B. Shrinking filter (0 if any 8-neighbor is 0)
	C. Smoothing filter (0 if 6 or more 8-neighbors are 0)

Results and Discussion

Related studies indicated (Kim et al., 2002b; Kim et al., 2003a; Lefcourt et al., 2003, 2005), and current findings confirmed, that fluorescence emissions in red band images due to chlorophyll *a* and chlorophyll-related compounds in the feces would be the most prominent fluorescence marker of fecal contamination. Results from these studies also indicated that taking the ratio of images at different wavebands could ameliorate problems related to heterogeneity of illumination and, further, that the effects of contamination could be amplified by taking advantage of the fact that contamination sites were brighter in red band images and equal or darker in blue or green band images compared to normal apple surfaces. However in this study, a general lack of dark areas corresponding to contamination sites and natural bright areas in blue or green band images limited their usefulness in ratio images or linear combinations of images (fig. 1). Thus, the analyses focused on detection of contamination sites in red band images. In a previous study (Lefcourt et al., 2003), gradient detection methods were used to reduce the effects of differences in intensity across individual red band images; these methods can be used to look at relative changes in intensity in 3 × 3 or 5 × 5 pixel areas. Differences in absolute intensity were addressed by adjusting thresholds based on intensity histograms of individual images. These techniques were the starting point for analyzing images in this study.

Image Intensity Scaling

To reduce the number of tests conducted, the relative advantages of median- and maximal-based intensity scaling were compared with the goal of selecting a single type of scaling for subsequent analyses. Testing indicated that the median option was more robust, in that small changes in the selected intensity or histogram levels for the upper transformation point did not influence detectability. In addition, comparisons of detection algorithms that included either no scaling, median-based scaling, or maximal-based scaling demonstrated that detection was greatest when the median option was used (table 2). In actuality, the maximal-based scaling performed very poorly, e.g., detection algorithms that included maximal-based scaling could not detect most of the

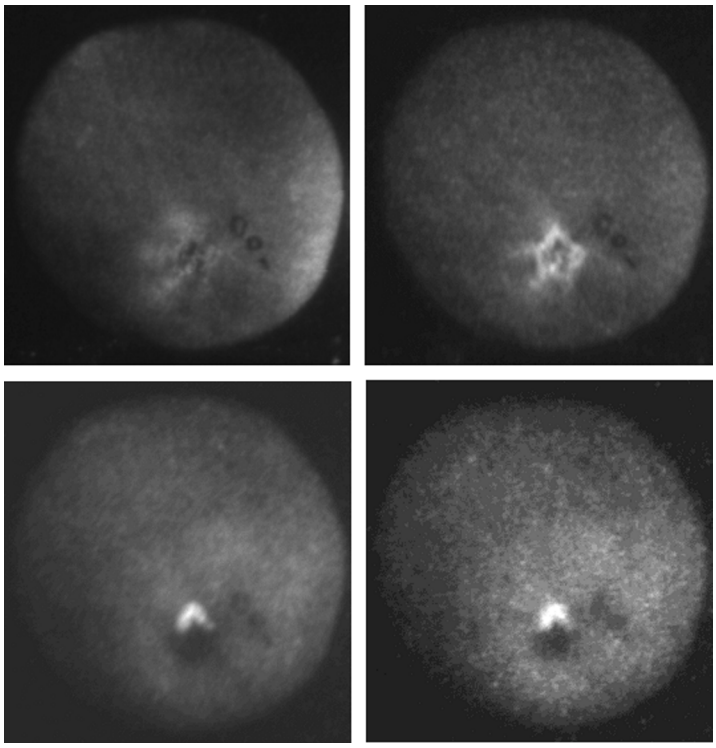

Figure 1. Clockwise from upper left are representative blue, green, far red, and red band fluorescence images of an apple treated with the 1:20 dilution of dairy feces from Beltsville. The lettering near the calyx is for identification. The bright inverted "v" in the sepal region of the red and far-red band images represents the fecal contamination site. Note in the blue and green band images the lack of indication of the fecal contamination site and the naturally bright areas.

Table 2. Number of contamination sites detected on apples treated with either 1:20 or 1:200 dilutions of feces, and number of sites detected when the area detection threshold for each filtering strategy was set to exclude all false positives. Using linear scaling based on the median histogram intensity of images resulted in better detection compared to using the near-maximal histogram intensity. In addition, detection was better with the Prewitt gradient filter compared to using a simple threshold filter.

	1:20 Dilution (n = 60)		1:200 Dilution (n = 47)	
Filtering Strategy	Detected	No False Positives	Detected	No False Positives
1. Median linear scaling 2. Binary threshold 175	47	0	26	0
1. 5 × 5 Prewitt 2. Median linear scaling 3. Binary threshold 225	60	60	40	32
1. Maximal linear scaling 2. Binary threshold 175	32	0	15	0
1. 5 × 5 Prewitt 2. Maximal linear scaling 3. Binary threshold 225	17	0	28	2
1. 5 × 5 Prewitt 2. Binary threshold 225	56	25	15	5

contamination sites when thresholds were set to eliminate all false positives. Subsequent tests used either no scaling or median-based intensity scaling.

1:20 Dilutions

Contamination sites for all 20 apples artificially contaminated with 1:20 dilutions of feces could be detected with no false positives using a number of detection schemes with one exception (fig. 2). The exception relates to a few apples that appeared to have natural contamination sites. By applying stringent selection parameters, the natural contamination sites for all but two apples could be excluded from detection. For the two remaining exceptions, the intensities of the natural sites were much greater than that of the artificial sites and thus were unlikely to be the result of cross-contamination during feces application. It should be noted that detection based on a simple binary threshold was very poor, and that detection was greatly enhanced by intensity scaling based on the median value of intensity histograms (table 1). Neither storage time after application nor washing had any meaningful impact on detectability.

1:200 Dilutions

Detection of 1:200 contamination sites was much more difficult compared to 1:20 sites; the area of contamination was smaller and less intense (fig. 3). For feces from Beltsville, no indication of contamination could be seen either before or after washing for one of the 10 treated apples; for feces from Clarksville, visually identifiable contamination was not apparent for four of the 10 apples. Apparently, the petals associated with the sepal area completely obscured the contamination sites of these five apples. This may be partially due to the much lower viscosity of the 1:200 dilutions compared to the 1:20 dilutions of feces. The dilutions were applied at the edge of the petals, and during application, it was noticed that the 1:200 dilution had a greater tendency to slide under the petals.

Table 3 shows the number of contamination sites detected for the 1:200 dilution by source of feces on day 1, day 7, and after washing. As the purpose of this comparison was to examine the effects of time and washing, the five apples with no visually detectable contamination were excluded from the tabulated results. The results are based on the use of the most effective strategy for detecting contamination (see below). Detection was slightly lower for feces from Clarksville, and detection was slightly reduced after washing, 58% versus 75%, respectively.

Optimizing the Detection Strategy

Successful detection of 1:200 contamination sites required extensive optimization of detection strategies. In initial tests, filter parameters and threshold values were varied broadly. Subsequently, for the more promising filtering strategies, optimal conditions were determined that allowed detection of the greatest number of contamination sites and the greatest number of sites with no false positives. False positives automatically excluded from consideration included detection of the edges of the lettering applied to apples for identification, detection at the edges of apples, a small number of what appeared to be natural contamination sites, and two sites that had healing cuts. A comparison of the efficacy of some of the optimized filtering strategies is

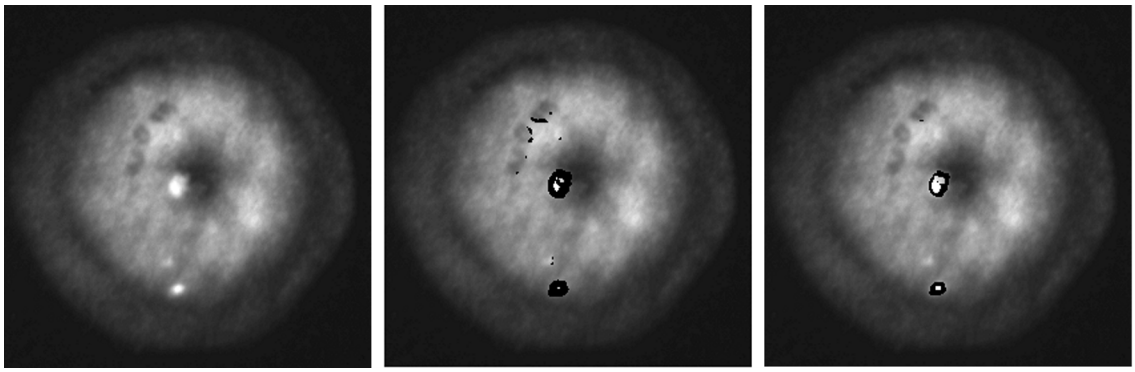

Figure 2. The bright spot in the middle of these red band images is the site where the apple was artificially contaminated with the 1:20 dilution of dairy feces from Clarksville. All three images were scaled using the median-based linear scaling function. The black areas in the middle image show the result of applying a 5 × 5 Prewitt filter and a binary image transformation threshold of 175, and then overlaying the result onto the original image. The image on the right shows the effect of shrinking to reduce detection of false positives (including the edges of letters used for identification). The bright spot in the bottom middle of the apple image appears to be a natural contamination site.

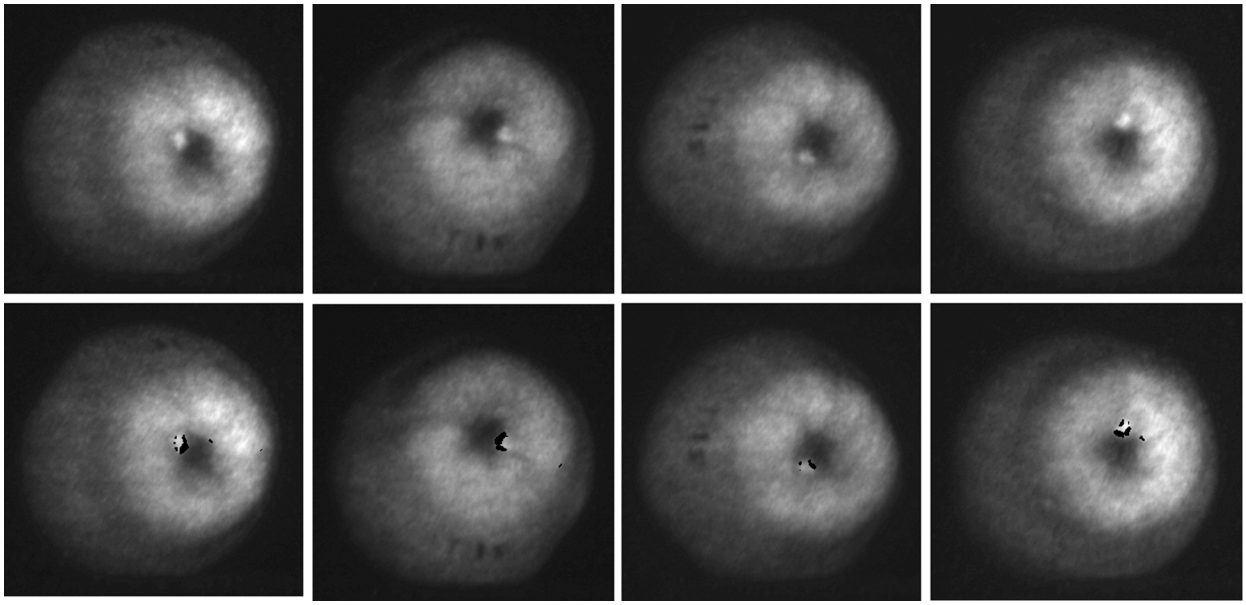

Figure 3. Detection of a 1:200 dilution contamination site on a single apple. Shown from left to right are red band images taken at four rotations. The bottom row shows pixels detected using a 5 × 5 Prewitt filter, median linear scaling, and a binary threshold of 200 overlaid on the original images in black. This apple is one of four apples treated with 1:200 dilutions that showed the effect on intensity of the contamination site as a function of rotation.

shown in table 4. In general, averaging filters marginally lessened detection, as did binning images. This finding indicates that detection sensitivity increases with increased pixel resolution.

Gradient filters were much superior to simple threshold filters, and the 5 × 5 Prewitt filter performed better than the 3 × 3 Prewitt filter. The performance of the 5 × 5 Sobel filter was similar to that of the 5 × 5 Prewitt filter. The greatest sensitivity resulted from using a lower value for the binary conversion threshold along with a higher value for the area detection threshold. For the binned images, shrinking along with a lower area detection threshold performed similarly to no shrinking along with a higher area detection threshold. For all filtering strategies, using higher area detection thresholds was found to be preferable to using an averaging filter. The most effective strategy used no binning, no averaging filter, a 5 × 5 Prewitt gradient filter, median-based linear scaling, a binary transformation threshold of 200, no shrinking or smoothing, and an area detection threshold of 42 pixels.

Table 3. Number of contamination sites detected on apples treated with 1:200 dilutions of feces 1 day and 7 days after application, and after washing. The filtering strategy used a 5 × 5 Prewitt gradient filter, median-based linear scaling, binary transformation using a threshold of 200, and an area detection threshold of 42 pixels.

	Time of Detection		
Source of Feces	Day 1	Day 7	After wash
Feces from Beltsville			
Total number	9	9	9
Total detected	9	9	9
Total with no false positives	8	8	8
Feces from Clarksville			
Total number	7	7	6
Total detected	7	4	4
Total with no false positives	4	4	3
All Feces			
Total number	16	16	15
Total detected	16	13	12
Total with no false positives	12	12	11

Effects of Rotating Apples for Imaging

Rotating apples was found to have a small effect on the intensity of imaged contamination sites. The effect was pronounced for only four of the 15 apples treated with 1:200 dilutions of feces where a response was detectable. An example of this phenomenon is shown in figure 3. In only one case did rotation prevent detection. For that apple, the contamination site was detectable for three of the four rotations.

Reflectance Images

In no case were contamination sites discernible in reflectance images. However, it must be emphasized that

Table 4. Number of contamination sites detected on apples treated with either 1:20 or 1:200 dilutions of feces, and number of sites detected when the area detection threshold for each filtering strategy was set to exclude all false positives. Comparison of optimized filtering strategies.

	1:20 Dilution (n = 60)		1:200 Dilution (n = 47)	
Filtering Strategy	Detected	No False Positives	Detected	No False Positives
1. 3 × 3 Prewitt 2. Median linear scaling 3. Binary threshold 225	60	56	40	26
1. Bin images 2 × 2 2. 3 × 3 Prewitt 3. Median linear scaling 4. Binary threshold 225	60	57	38	24
1. 5 × 5 Prewitt 2. Median linear scaling 3. Binary threshold 200	60	60	41	35
1. 5 × 5 Sobel 2. Median linear scaling 3. Binary threshold 200	60	60	41	33
1. 5 × 5 averaging 2. 5 × 5 Prewitt 3. Median linear scaling 4. Binary threshold 200	60	56	47	28

optimal wavelengths for imaging apples for detection of fecal contamination extend into the near IR (Kim et al., 2002a). In this study, the longest wavelength was the far-red band (730 nm).

Practical Considerations

Results from this study highlight a number of issues related to detection of fecal contamination of apples. First, the common sense-based impression that it will be harder to detect fecal contamination of the apple calyx compared to other apple surfaces proved to be valid. Very low levels of contamination (<15 ng) that, in a prior study (Lefcourt et al., 2003), could be detected on cheek surfaces of apples could not be seen or were harder to detect in this study, which examined contamination of the calyx region. This difference in detectability raises the issue of whether to design commercial systems for best obtainable detection sensitivity with the realization that sensitivities will differ according to where on the apple the contamination occurs or, alternatively, to select a sensitivity threshold that can be universally applied to all apple surfaces. Detection of the 1:20 dilution (approximately 150 ng of dry matter) was near 100% for cheek apple surfaces tested in the previous study (Lefcourt et al., 2003) and was 100% in this study. If a detection limit of 150 ng was adopted for commercial use, this level of contamination could be detected with a number of different detection algorithms using reduced levels of sensitivity. In this study, with this reduced sensitivity, false positives due to edges could be eliminated and those due to naturally occurring contamination sites could be reduced to the two apples with sites that were brighter than the treatment sites.

Another issue of concern is variability of illumination. Use of a randomized fiber-optic bundle instead of a divergent lens to expand the laser beam for illumination would effectively minimize the heterogeneity of illumination across samples. With this modification, frequency-domain analyses of images might prove useful for detection.

Detection in this study could have been improved by taking into consideration the shape of the contamination sites. The sites with the lowest level of contamination were almost always near-circular in shape. This option was not pursued, as the potential range of shapes for naturally occurring contamination sites is unknown.

The ability to reliably detect fecal contamination consisting of 150 ng of dry matter in the calyx of the apple using laser-induced fluorescence responses suggests that this methodology may be useful for development of commercial screening systems. Such systems would be useful for screening apples destined for either juice making or the fresh produce market. The economic viability of such systems could be enhanced by also incorporating techniques to measure apple quality.

Conclusions

The laser-induced fluorescence imaging technique was found to be a sensitive method for detecting fecal contamination of the apple calyx. The major obstacle for detecting 1:200 dilution of dairy feces was the obstruction of both the illumination path and sensor view of contamination sites by sepal petals; the low viscosity of the 1:200 dilution allowed the diluted feces to slide under the petals. However, 100% of the sites contaminated with 1:20 dilutions of dairy feces (<150 ng of dry matter) could easily be detected. For the sites contaminated with 1:200 dilutions of feces, 25% showed no evidence of contamination, presumably due to obstruction by the petals. For the other 75% of the apples with visual signs of contamination, 75% of the contamination sites could be detected prior to washing, and 58% after washing. Results suggest that this technology is a viable candidate for the development of commercial systems to detect fecal contamination of apples.

References

Armstrong, G. L., J. Hollingsworth, and J. G. Morris, Jr. 1996. Emerging foodborne pathogens: *Escherichia coli* O157:H7 as a model of entry of a new pathogen into the food supply of the developed world. *Epidemiol. Rev.* 18(1): 29-51.

Besser, R. E., S. M. Lett, J. T. Weber, M. P. Doyle, T. J. Barret, J. G. Wells, and P. M. Griffin. 1993. An outbreak of diarrhea and hemolytic uremic syndrome from *Escherichia coli* 0157:H7 in fresh pressed apple cider. *JAMA* 269(17): 2217-2220.

Brackett, R. E. 1999. Incidence, contributing factors, and control of bacterial pathogens in produce. *Postharvest Biol. Tech.* 15(3): 305-311.

Buchanan, R. L., and M. P. Doyle. 1997. Foodborne disease significance of *Escherichia coli* 0157:H7 and other enterohemorrhagic *E. coli*. *Food Tech.* 51(10): 69-76.

CDC. 1996. Outbreak of *E. coli* 0157:H7 infections associated with drinking unpasteurized commercial apple juice - October 1996. *MMWR* 45(44): 975-982.

CDC. 1997. Outbreaks of *Escherichia coli* 0157:H7 infection and cryptosporidiosis associated with drinking unpasteurized apple cider - Connecticut and New York, October 1996. *MMWR* 46(1): 4-8.

Cody, S. H., M. K Glynn, J. A. Farrar, K. L. Cairns, P. M. Griffin, J. Kobayashi, M. Fyfe, R. Hoffman, A. S. King, J. H. Lewis, B. Swaminathan, R. G. Bryant, and D. J. Vugia. 1999. An outbreak of *Escherichia coli* O157:H7 infection from unpasteurized commercial apple juice. *Annals of Internal Med.* 130(3): 202-209.

FDA. 2001. Hazard analysis and critical control point (HAACP); Procedures for the safe and sanitary processing and importing of juices. *Federal Registry* 66(13): 6137-6202.

Kim, M. S., A. M. Lefcourt, K. Chao, Y.-R. Chen, I. Kim, and D. Chan. 2002a. Multispectral detection of fecal contamination on apples based on hyperspectral imagery: Part I. Application of visible and near-infrared reflectance imaging. *Trans. ASAE* 45(6): 2027-2037.

Kim, M. S., A. M. Lefcourt, Y.-R. Chen, I. Kim, D. Chan, and K. Chao. 2002b. Multispectral detection of fecal contamination on apples based on hyperspectral imagery: Part II. Application of hyperspectral fluorescence imaging. *Trans. ASAE* 45(6): 2039-2047.

Kim, M. S., A. M. Lefcourt, and Y.-R. Chen. 2003a. Optimal fluorescence excitation and emission bands for detection of fecal contamination. J. Food Prod. 66(7): 1198-1207.

Kim, M. S., A. M. Lefcourt, and Y.-R. Chen. 2003b. Multispectral laser-induced fluorescence imaging system for large biological samples. Applied Optics 42(19): 3927-3934.

Lang, M. M., S. C. Ingham, and B. H. Ingham. 1999. Verifying apple cider plant sanitation and hazard analysis critical control point programs: Choices for indicator bacteria and testing. J. Food Protect. 62(8): 887-893.

Lefcourt, A. M., M. S. Kim, and Y.-R. Chen. 2003. Automated detection of fecal contamination of apples by multispectral laser-induced fluorescence imaging. Applied Optics 42(19): 3935-3943.

Lefcourt, A. M., M. S. Kim, and Y.-R. Chen. 2005. Detection of fecal contamination of apples with nanosecond-scale time-resolved imaging of laser-induced fluorescence. Applied Optics 44(7): 1160-1170.
Mead, P. S., L. Slutsker, V. Dietz, L. F. McCaig, J. S. Bresee, C. Shapiro, P. M. Griffin, and R. V. Tauxe. 1999. Food-related illness and death in the United States. Emerging Infectious Diseases 5(6): 607-625.
Riordan, D. C. R., G. M. Sapers, T. R. Hankinson, M. Magee, A. M. Mattrazzo, and B. A. Annous. 2001. A study of U.S. orchards to identify potential sources of Escherichia coli 0157:H7. J. Food Protect. 64(9): 1320-1327.
Steele, B. T., N. Murphy, G. S. Arbus, and C. P. Rance. 1982. An outbreak of hemolytic uremic syndrome associated with the ingestion of fresh apple juice. J. Pediatr. 101(6): 963-965.
Uljas, H. E., and S. C. Ingham. 2000. Survey of apple growing, harvesting, and cider manufacturing practices in Wisconsin: Implications for safety. J. Food Safety 20(2): 85-100.
Weeks Jr., A. R. 1996. Fundamentals of Electronic Image Processing. Bellingham, Wash.: SPIE Optical Engineering Press.